# Development of a Split Fluorescent Protein-Based RNA Live-Cell Imaging System to Visualize mRNA Distribution in Plants

**Nien-Chen Huang**
Institute of Plant and Microbial Biology Academia Sinica
**Kai-Ren Luo**
Institute of Plant and Microbial Biology Academia Sinica
**Tien-Shin Yu** ( tienshin@gate.sinica.edu.tw )
Institute of Plant and Microbial Biology Academia Sinica https://orcid.org/0000-0003-3395-1809

**Research Article**

**Keywords:** RNA live-cell imaging, MCP, PCP, split fluorescent proteins, puncta distribution of mobile mRNAs, agro-infiltration

**Posted Date:** October 28th, 2021

**DOI:** https://doi.org/10.21203/rs.3.rs-994002/v1



**Version of Record:** A version of this preprint was published at Plant Methods on February 8th, 2022. See the published version at https://doi.org/10.1186/s13007-022-00849-3.

# Abstract

**Background:** RNA live-cell imaging systems have been used to visualize subcellular mRNA distribution in living cells. The MS2-based RNA imaging system exploits the coat protein (MCP) of MS2 bacteriophage with RNA-binding activity and the RNA hairpin structure MS2 binding sequences (MBS) recognized by MCP to indirectly label mRNAs. Co-expression of fluorescent protein (FP)-fused MCP and target mRNA conjugated with multiple copies of MBS allows for visualizing of mRNA localization by confocal microscopy. To minimize the background fluorescence in cytosol, the nucleus localization sequence was used to sequester the MCP-FP not bound to mRNA in the nucleus. However, strong fluorescence in the nucleus may limit the application of RNA visualization in the nucleus and sometimes may interfere in detecting fluorescence signals in cytosol, especially in cells with low signal-to-noise ratio.

**Results:** By using the split FP-based approach, we eliminated the background fluorescence derived from MCP-FP not bound to mRNAs. MCP and PCP, a coat protein of PP7 bacteriophages with RNA-binding activity, were fused with the N- or C-terminus of split FPs ($FP_N$ or $FP_C$). On co-expression of MCP-$FP_N$ and PCP-$FP_C$ with the target mRNA conjugated with multiple copies of the hairpin structure recognized by MCP and PCP, the interaction of RNA and proteins can bring split FPs together to reconstitute functional FPs that allow for visualizing target mRNAs in living cells. We optimized the combinations of MCP- and PCP-FPs with minimal background fluorescence and applied the imaging system to visualize mRNAs in living plant cells.

**Conclusions:** We established a background-free RNA live-cell imaging system that provides a platform to visualize subcellular mRNA distribution in living plant cells.


# Background

Most cells transport mRNAs to specific subcellular compartments for localized RNA translation. Instead of transporting a quantity of proteins, the transport of mRNA provides an efficient strategy to distribute proteins to specific subcellular compartments. In eukaryotic cells, asymmetric mRNA localization is a conserved mechanism to create translation hotspots for regulating spatial gene expression in response to environmental cues [1]. The intracellular mRNA asymmetric distribution in plants can be extended to the intercellular level in which specific plant mobile mRNAs are transcribed in local tissues and undergo long-distance movement through phloem to exert non-cell autonomous functions, including regulation of leaf development [2], floral transition [3, 4], and potato tuber formation [5]. Thus, understanding the mRNA subcellular distribution may provide information to unravel RNA logistics and post-transcriptional gene regulation.

In living plant cells, directly visualizing mRNAs by microscopy is a challenge task. Many approaches have been developed to allow for visualizing mRNAs in living cells. Directly labeling mRNAs can be achieved by incorporating *in vitro*-synthesized mRNA with fluorescein-labeled nucleotides or introduce molecular beacons into cells to allow the detection of fluorescein-labeled mRNAs or mRNAs specifically hybridized

with molecular beacons [6, 7]. However, these *in vitro* RNA labeling systems require invasive injection of labeled RNA into plant cells such as by microinjection or particle bombardment. In addition, the *in vitro*-synthesized RNAs may behave differently from the *in vivo* RNAs because the RNA synthesized *in vitro* may bypass the RNA modification occurring in nucleus, which may change the properties of RNA.

Alternatively, RNA can be indirectly visualized by an RNA aptamer-based approach. In this system, the target mRNA is genetically modified by tagging with an RNA aptamer recognized by RNA-binding proteins (RBPs). Co-expression of fluorescent proteins (FPs) conjugated with RBPs with aptamer-tagged mRNA allows for indirectly labelling mRNA in living cells. MCP, a coat protein derived from MS2 bacteriophage with RNA-binding activity, and the stem loop structures recognized by MCP have been widely used to monitor mRNA localization in yeast, fruit fly, mammals and plants [8-13]. To reduce the background GFP fluorescence detected in the cytosol, the nucleus localization sequence (NLS) has been used to sequester the MCP-GFP not bound to RNA in the nucleus [8, 13]. In addition, the signal-to-noise ratio of RNA detected in the cytosol can be greatly improved by using the plant-specific NLS tightly restricts MCP in the nucleus [13]. Although the MCP-based approach has been successfully used to visualize the intracellular distribution of mobile and non-mobile mRNA in plants [13], the background GFP fluorescence derived from nucleus-localized MCP-GFP may interfere in detecting mRNA with low expression level. In addition, cells that undergo active cell division are smaller and the nucleus is relatively large [14], so the high nucleus-to-cytoplasmic ratio may disturb the detection of RNA localization due to strong background GFP fluorescence in the nucleus.

Here, we improved the RNA live-cell imaging system to reduce the background fluorescence in the nucleus by using a split FP-based approach. We conjugated split FPs with bacterial phage MS2 or PP7 coat protein (MCP or PCP, respectively). The target mRNA was flanked with the MS2 binding sites (MBS) and PP7 binding sites (PBS) in tandem repeats [15]. The fluorescence only shines when split MCP-FP and PCP-FP binds to the mRNA-MBS-PBS that bring two split proteins together to reconstitute a mature FP.

# Results And Discussion

### Development of split FP-based RNA live-cell imaging system

To develop the mRNA live-cell imaging system without background GFP fluorescence in the nucleus, we exploited the bimolecular fluorescence complementation (BiFC) system to reduce background GFP fluorescence derived from MCP-GFP not bound to mRNA. In this system, two different RNA-binding proteins (RBPs) were fused with N- or C-terminus of split FPs, respectively, to reduce the fluorescence produced from RBP-FPs not bound to mRNA. The interaction between RBPs and RNA motifs recognized by RBPs may bring two different split FPs together to allow the detection of fluorescence (Figure 1A). We selected two coat proteins of bacteriophages, MCP and PCP, which specifically bind to a RNA hairpin structure of MBS or PBS, respectively [15]. MCP and PCP were conjugated with the N-terminus ($FP_N$, amino acids 1-173 from Venus) or C-terminus ($FP_C$, amino acids 156-239 from SCFP3A) fragment of the split FP protein [16]. To identify the optimized fusion proteins for the system, we generated different

MCP/PCP-FP fusion proteins by flanking $FP_N$ or $FP_C$ with MCP or PCP (Figure 1B). In addition, the NLS derived from Arabidopsis FD [13] was used to locate MCP or PCP to the nucleus (Figure 1B). To generate the target mRNAs that can be recognized by MCP and PCP, the fragments containing 12 copies of MBS-PBS tandem repeats were conjugated with *FT* or *RFP* cDNA to create $FT_{HSL12}$ (*FT*-hybrid stem loops, 12 copies) or $RFP_{HSL12}$, respectively (Figure 1A).

## Background GFP fluorescence was under the detection limit in cells expressing MCP-$FP_N$ and PCP-$FP_C$

To identify the combinations of MCP and PCP with a minimal background GFP fluorescence in plant cells, we transiently expressed different MCP- and PCP-split FPs in leaves of 3-weak-old *Nicotiana benthamiana* by agro-infiltration and examined GFP fluorescence under a confocal laser scanning microscope at 3 days after infiltration. When NLS-containing $M_{NLS}$-$FP_N$ was co-expressed with P-$FP_C$ or $FP_C$-P, weak GFP fluorescence was detected in both cytosol and nucleus (Figure 2A-D), which suggests that the separation of MCP and PCP into different subcellular compartments may not significantly reduce the background GFP fluorescence. Consistently, when NLS-containing $P_{NLS}$-$FP_C$ was co-expressed with $FP_N$-M, the background GFP fluorescence was again detected in the cytosol and nucleus (Figure 3A, 3D, 3G). However, when $P_{NLS}$-$FP_C$ was co-expressed with M-$FP_N$ or NLS-containing $M_{NLS}$-$FP_N$, the background GFP fluorescence that formed a speckle-like spot was detected only in the nucleus (Figure 3B-C, 3E-F, 3H-I), which suggests that the topology of fusion proteins rather than subcellular localization may contribute to the background GFP fluorescence.

We next examined background GFP fluorescence in cells expressing MCP-FP and PCP-FP without NLS. When M-$FP_N$ was co-expressed with P-$FP_C$, we consistently obtained the images without detectable background GFP fluorescence (Figure 4A and 4E). However, the other 3 combinations of MCP-FP and PCP-FP conferred weak (Figure 4B and 4F) or strong GFP fluorescence (Figure 4C-D, and 4G-H). We summarize these results in Table 1. Taken together, our results revealed that the combination of MCP-$FP_N$ and PCP-$FP_C$ produced undetectable background GFP fluorescence. In addition, the combination of $P_{NLS}$-$FP_C$ with M-$FP_N$ or $M_{NLS}$-$FP_N$ produced a speckle-like background GFP fluorescence in the nucleus, which may also provide a useful positive control for presence of the infiltrated constructs.

## Detection of mRNA localization in background-free split FP-based imaging system

To verify the application of the split-FP system for localization of mRNAs, we co-infiltrated M-$FP_N$ and P-$FP_C$ with $FT_{HSL12}$ or $RFP_{HSL12}$, two mRNAs with a differential subcellular distribution pattern [13] in tobacco leaves. At 3 days after infiltration, no fluorescence was detected in control cells co-expressing M-$FP_N$ and P-$FP_C$ without mRNA (Figure 5A, 5E). However, GFP fluorescence was detected in the cytosol of cells co-expressing M-$FP_N$ and P-$FP_C$ with $RFP_{HSL12}$ or $FT_{HSL12}$ mRNA. Of note, the fluorescence in the cytosol showed distinct distribution patterns in cells expressing $RFP_{HSL12}$ or $FT_{HSL12}$ mRNA: in cells expressing $RFP_{HSL12}$, the fluorescence was evenly distributed at the cell periphery (Figure 5B, 5F), whereas with $FT_{HSL12}$, the fluorescence showed a punctate distribution (Figure 5C, 5G). These subcellular

distribution patterns were reminiscent of the previous MS2-based mRNA live-cell imaging [13]. However, in the split FP-based imaging system, the GFP fluorescence spots were detected inside or in the boundary of the nucleus (Figure 5D-H), which were not detected in the previous MS2-based system [13]. These results suggest the broader use of a split FP-based imaging system for visualizing mRNA distribution.

We further verify the application of the split FP-based imaging system with speckle-like background GFP fluorescence for mRNA visualization. In control cells co-expressing $M_{NLS}$-$FP_N$ and $P_{NLS}$-$FP_C$, speckle-like GFP fluorescence was detected in the nucleus (Figure 6A and 6C), whereas in cells co-expressing $M_{NLS}$-$FP_N$ and $P_{NLS}$-$FP_C$ with $FT_{HSL12}$ mRNA, the GFP fluorescence was detected in the cytosol with a puncta distribution pattern (Figure 6B and 6D). Of note, the GFP fluorescence spots were detected in the nucleus (Figure 6D), suggesting that the speckle-like background GFP may not greatly disturb mRNA visualization in the nucleus (Figure 5B, 5D).

# Methods

### Plant materials and growth conditions

*Nicotiana benthamiana* plants were grown in a growth chamber under 27$^{o}$C, 16-h/8-h day/night cycles and light intensity of 100 mmol $m^{-2}$ $s^{-1}$. The 3-week-old plants were used for agro-infiltration assay.

### Plasmid construction and Arabidopsis transformation

The DNA fragments of MCP and PCP were PCR-amplified with the following primers: MCP-For (5'-GGATCCATGGCTTCTAACTTTACTCAGTTCG-3'), MCP-Rev (5'-CTCGAGGTAGATGCCGGAGTTTGCTGCGATT-3'), PCP-For (5'-GGATCCATGTCCAAAACCATCGTTCTTTCGG-3'), PCP-Rev (5'-CTCGAGACGGCCCAGCGGCACAAGGTTGACG-3'). The DNA fragments of MCP and PCP were confirmed by sequencing and cloned into split FP-containing binary vectors pVYNE, pVYNE(R), pSCYCE, or pSCYCE(R) [16] to generate M-$FP_N$, $FP_N$-M, P-$FP_C$ and $FP_C$-P, respectively. The C-terminal fragment (211-240 a.a.) of Arabidopsis FD, which contains the nucleus localization sequence (NLS) [13], was inserted in M-$FP_N$ or P-$FP_C$ to generate $M_{NLS}$-$FP_N$ and $P_{NLS}$-$FP_C$, respectively.

For the 12 copies of the MBS-PBS hybrid stem loop sequence (HSL12), the Pcr4-12X-MBS-PBS [15] DNA was digested with BamHI and SpeI, followed by the Klenow fill-in reaction. The 1402-bp HSL12 fragment was gel-eluted and ligated with the binary vector pCAMBIA1390 that contains the *35S-FT* or *35S-RFP* to form the p1390-35S-$FT_{HSL12}$ or p1390-35S-$RFP_{HSL12}$ construct, respectively.

### Agro-infiltration of *N. benthamiana*

*Agrobacterium tumefaciens* strain AGL1 carrying individual constructs was cultured in 20 mL LB broth (10 g/L Tryptone, 5 g/L yeast extract, 10 g/L NaCl) containing 50 mg $mL^{-1}$ kanamycin, 10 mM MES, pH 5.7 and 20 mM acetosyringone at 28$^{o}$C with 220 rpm shaking for 2 days. Bacteria were pelleted by

centrifugation and resuspended in infiltration medium (10 mM MgCl2, 10 mM MES, pH 5.7, and 200 mM acetosyringone) to OD600 = 1.0. The bacterial solution was placed at room temperature for at least 1 h. For agro-infiltration, bacteria solution was infiltrated into the abaxial side of the $4^{th}$ or $5^{th}$ leaves of 3-week-old *N. benthamiana* by using a needle-removed 5-mL syringe. For co-infiltration with 2 or 3 different constructs, different bacterial solution or infiltration medium was mixed at a 1:1 volume ratio and infiltrated into leaves. The infiltrated plants were cultured in growth chambers for 3 days, then infiltrated leaves were excised for confocal laser scanning microscopy.

### Confocal laser scanning microscopy

GFP fluorescence was observed by confocal laser scanning microscopy (LSM880, Carl Zeiss) with the argon laser was set to 488/500-530 for excitation/emission.

## Abbreviations

BiFC: bimolecular fluorescence complementation

MCP: MS2 bacteriophage coat protein

PCP: PP7 bacteriophage coat protein

MBS: MCP binding sequences

PBS: PCP binding sequences

FP: fluorescent protein

NLS: nucleus localization sequence

## Declarations

### Acknowledgements

We would like to thank Mrs. Mei-Jane Fang for assistance in troubleshooting the confocal microscopy.

### Authors' contributions

NCH and TSY planed the research. NCH carried out experiments and drafted the manuscript. KRL carried out experiments of RFP localization. TSY contributed to writing the manuscript. All authors read and approved the final manuscript.

### Funding

This work was supported by grants (MOST 108-2311-B-001-025-MY3) from the Ministry of Science and Technology, Taiwan and (AS-TP-108-L01) from Academia Sinica, Taiwan.

### Availability of data and materials

All data and materials are available upon request to TSY (tienshin@gate.sinica.edu.tw).

### Ethics approval and consent to participate

Not applicable.

### Consent for publication

All authors read and agreed to publish the final manuscript.

### Competing interests

The authors declare that they have no competing interests.

## References


1. Das S, Vera M, Gandin V, Singer RH, Tutucci E (2021) Intracellular mRNA transport and localized translation. Nat. Rev. Mol. Cell Biol. 22: 483-504

2. Haywood V, Yu TS, Huang NC, Lucas WJ (2005) Phloem long-distance trafficking of *GIBBERELLIC ACID-INSENSITIVE* RNA regulates leaf development. Plant J. 42: 49-68

3. Lu KJ, Huang NC, Liu YS, Lu CA, Yu TS (2012) Long-distance movement of Arabidopsis *FLOWERING LOCUS T* RNA participates in systemic floral regulation. RNA Biol. 9: 653-662

4. Huang NC, Jane WN, Chen J, Yu TS (2012) *Arabidopsis thaliana CENTRORADIALIS* homologue (*ATC*) acts systemically to inhibit floral initiation in Arabidopsis. Plant J. 72: 175-184

5. Banerjee AK, Chatterjee M, Yu Y, Suh SG, Miller WA, Hannapel DJ (2006) Dynamics of a mobile RNA of potato involved in a long-distance signaling pathway. Plant Cell 18: 3443-3457

6. Christensen N, Tilsner J, Bell K, Hammann P, Parton R, Lacomme C, Oparka K (2009) The 5' cap of tobacco mosaic virus (TMV) is required for viron attachment to the actin/endoplasmic reticulum network during early infection. Traffic 10: 536-551

7. Göhring J, Jacak J, Barta A (2014) Imaging of endogenous messenger RNA splice variants in living cells reveals nuclear retention of transcripts inaccessible to nonsense-mediated decay in Arabidopsis. Plant Cell 26:754-764

8. Buxbaum AR, Haimovich G, Singer RH (2015) In the right place at the right time: visualizing and understanding mRNA localization. Nat. Rev. Mol. Cell Biol. 16: 95-109

9. Bertrand E, Chartrand P, Schaefer M, Shenoy SM, Singer RH, Long RM (1998) Localization of ASH1 mRNA particles in living yeast. Mol. Cell 2: 437-445

10. Forrest KM, Gavis ER (2003) Live imaging of endogenous RNA reveals a diffusion and entrapment mechanism for nanos mRNA localization in Drodophila. Curr. Biol. 13: 1159-1168

11. Park HY, Lim H, Yoon YJ, Follenzi A, Nwokafor C, Lopez-Jones M, Meng X, Singer RH (2014) Visualization of dynamics of single endogenous mRNA labeled in live mouse. Science 343: 422-424

12. Hamada S, Ishiyama K, Choi S-B, Wang C, Singh S, Kawai N, Franceschi VR, Okita TW (2003) The transport of prolamine RNAs to prolamine protein bodies in living rice endosperm cells. Plant Cell 15: 2253-2264

13. Luo KR, Huang NC, and Yu TS (2018) Selective targeting of mobile mRNAs to plasmodesmata for cell-to-cell movement. Plant Physiol. 177: 604-614

14. Trombetta VV (1939) The nuclear ratio in developing plant cells. Am. J. Bot. 26: 519-529

15.Wu B, Chen J, and Singer RH (2014) Background free imaging of single mRNAs in live cells using split fluorescent proteins. Sci. Rep. 4: 3615

16. Waadt R, Schmidt LK, Lohse M, Hashimoto K, Bock R, and Kudla J (2008) Multicolor bimolecular fluorescence complementation reveals simultaneous formation of alternative CBL/CIPK complexes in planta. The Plant J. 56: 505-516

# Tables

Table 1. Summary of background GFP fluorescence detection with different combinations of split fluorescent proteins

| MCP varieties | PCP varieties | Background | Fluorescence |
|---|---|---|---|
| $M_{NLS}$-$FP_N$ | P-$FP_C$ | Yes | nucleus, cytosol |
| $M_{NLS}$-$FP_N$ | $FP_C$-P | Yes | nucleus, cytosol |
| $FP_N$-M | $P_{NLS}$-$FP_C$ | Yes | nucleus, cytosol |
| M-$FP_N$ | $P_{NLS}$-$FP_C$ | Yes | speckle in nucleus |
| $M_{NLS}$-$FP_N$ | $P_{NLS}$-$FP_C$ | Yes | speckle in nucleus |
| M-$FP_N$ | P-$FP_C$ | No | Non-detectable |
| $FP_N$-M | P-$FP_C$ | Yes | cytosol |
| M-$FP_N$ | $FP_C$-P | Yes | nucleus, cytosol |
| $FP_N$-M | $FP_C$-P | Yes | cytosol |

# Figures

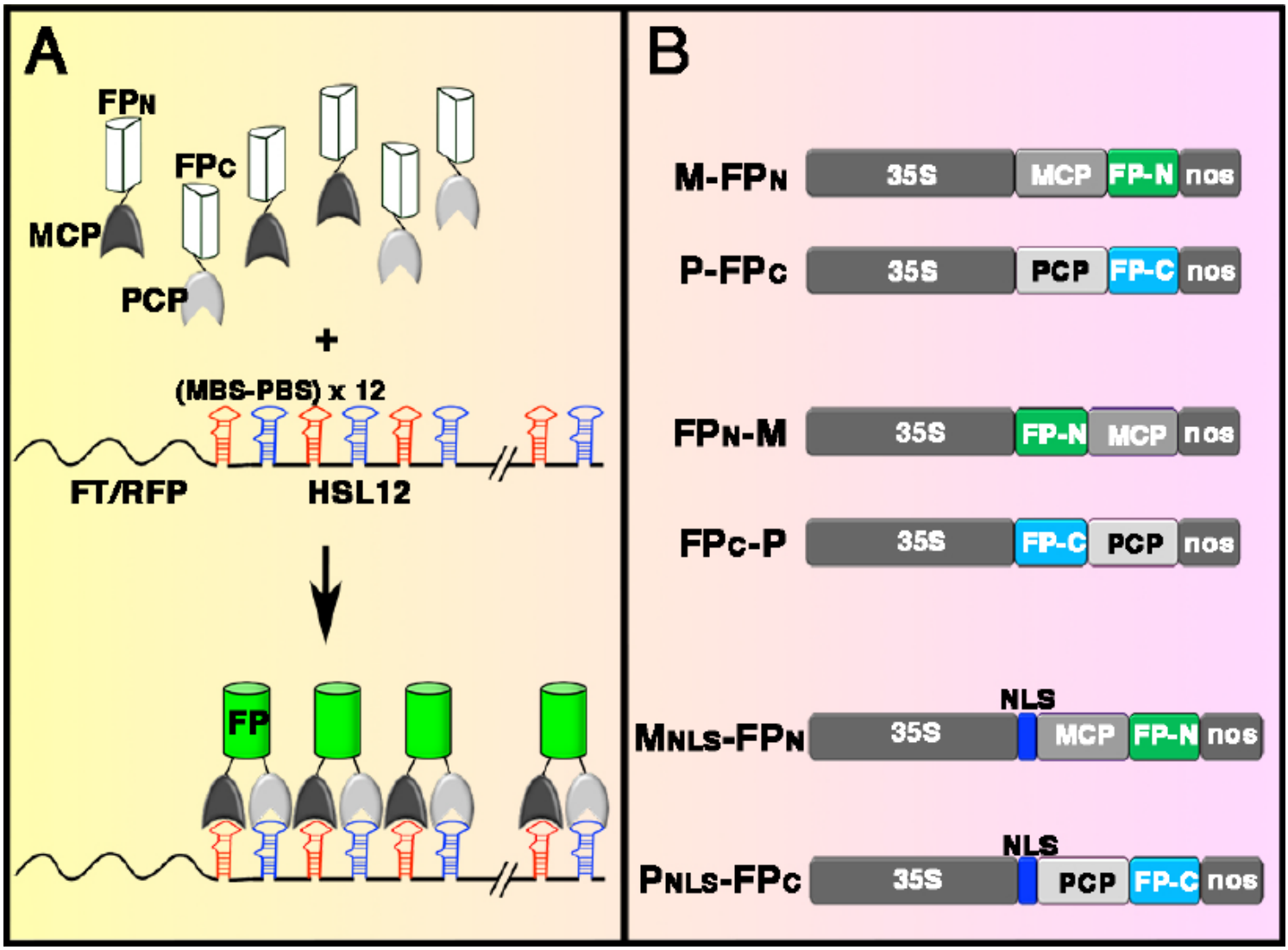


**Figure 1**

Illustration of split fluorescent protein-based RNA live-cell imaging system (A) MCP or PCP, coat proteins of MS2 or PP7 bacteriophage, respectively, was fused with the N- or C-terminus of split fluorescent protein (FP) FPN or FPC, respectively. The FT or RFP mRNA was conjugated with 12 copies of MBS-PBS, the hairpin structure recognized by MCP and PCP, to generate FTHSL12 or RFPHSL12 chimeric RNA. The binding of MCP and PCP with the hairpin structure of MBS-PBS brings two split FPs together to reconstitute the functional FP for indirect visualization of mRNAs in living cells. (B) Illustration of the constructs of MCP (M) or PCP (P) fused with the N- or C-terminus of FPN or FPC. The nucleus localization sequence (NLS) from Arabidopsis FD was inserted to sequester MCP- or PCP-FP fusion proteins in nucleus. The constructs were driven by a CaMV35S promoter and had an NOS terminator.

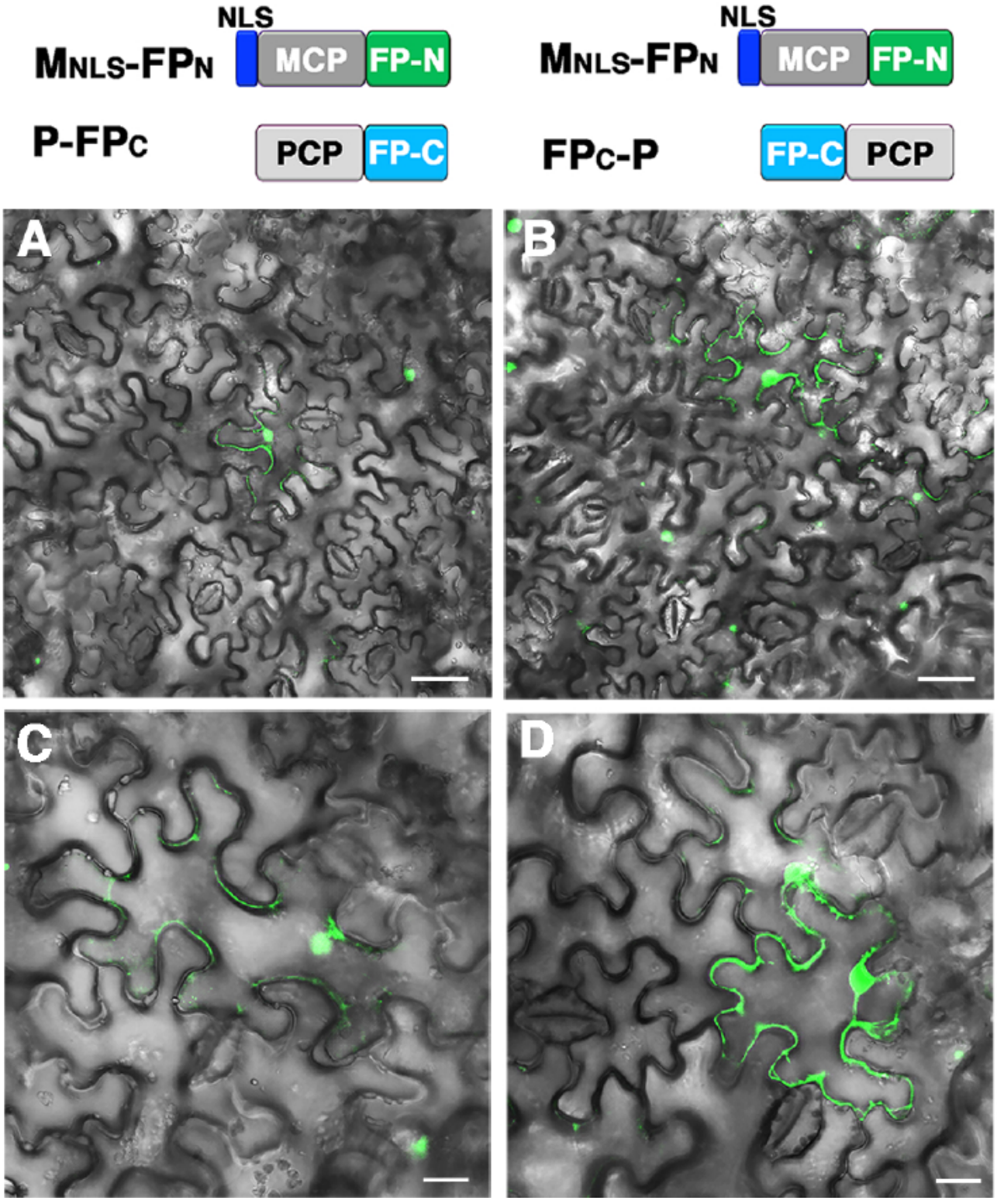


## Figure 2

Detection of background GFP fluorescence in cells with co-expression of PCP-FP and NLS containing MCP-FP Confocal microscopy of N. benthamiana leaves co-infiltrated with (A, C) MNLS-FPN and P-FPC or (B, D) MNLS-FPN and FPC-P. (C) and (D) Magnified images of (A) and (B), respectively. Note that background GFP fluorescent is detected in both cytosol and nucleus. Scale bar: (A) and (B) = 50 μm; (C) and (D) = 20 μm.

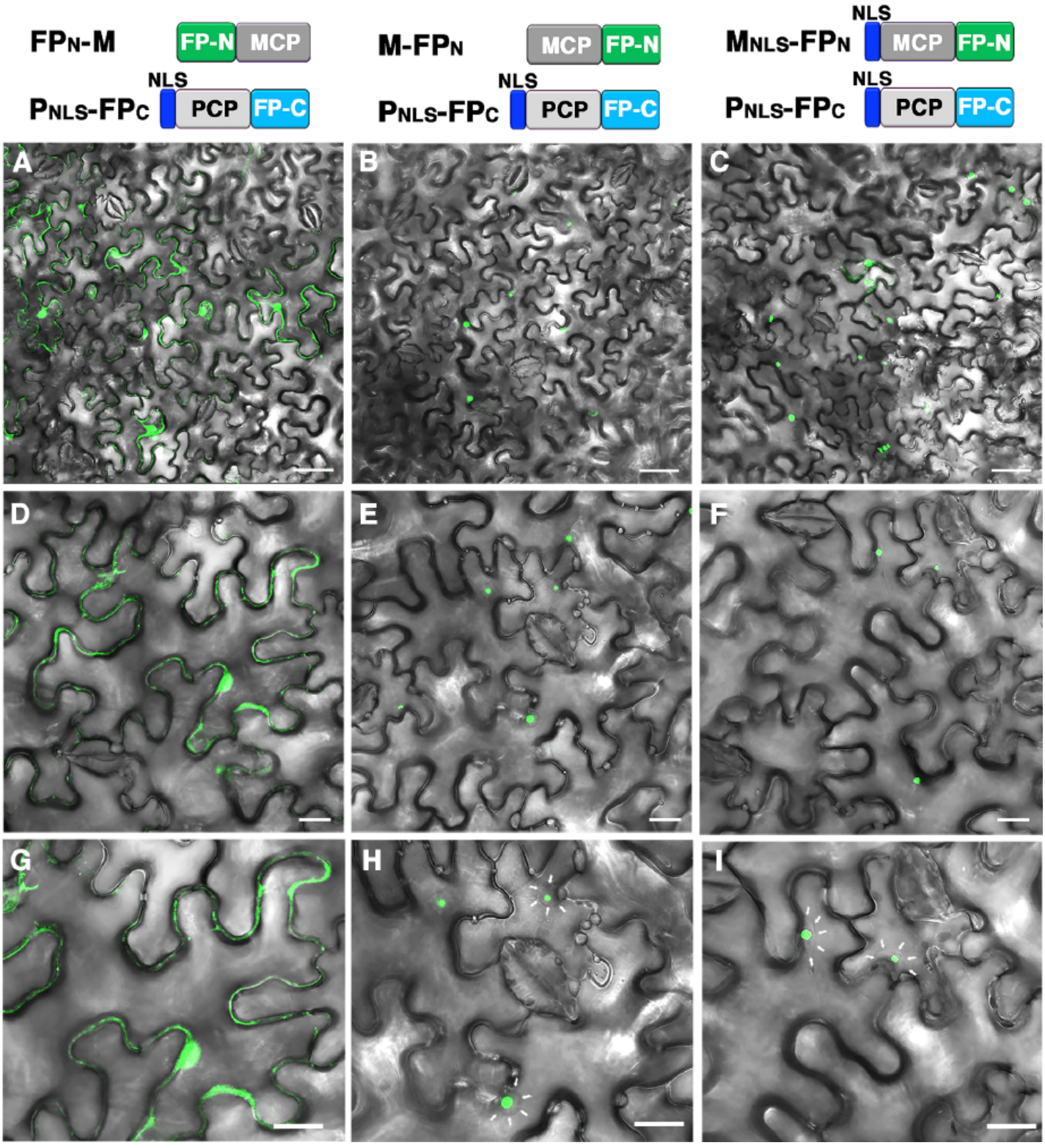


## Figure 3

Speckle-like background GFP fluorescence in nucleus of cells with co-expression of MCP-FP and NLS-containing PCP-FP Confocal microscopy of N. benthamiana leaves co-infiltrated with (A, D, G) FPN-M and PNLS-FPC; (B, E, H) M-FPN and PNLS-FPC; or (C, F, I) MNLS-FPN and PNLS-FPC. (D-I) Magnified images of (A-C). Note that the background GFP fluorescence is detected in both cytosol and nucleus in (A, D, G),

whereas the speckle-like background GFP fluorescence is detected in nucleus in (B-C, E-F, H-I). Scale bar: (A-C) = 50 μm; (D-I) = 20 μm. The boundary of nucleus is indicated by white arrows in (H) and (I).

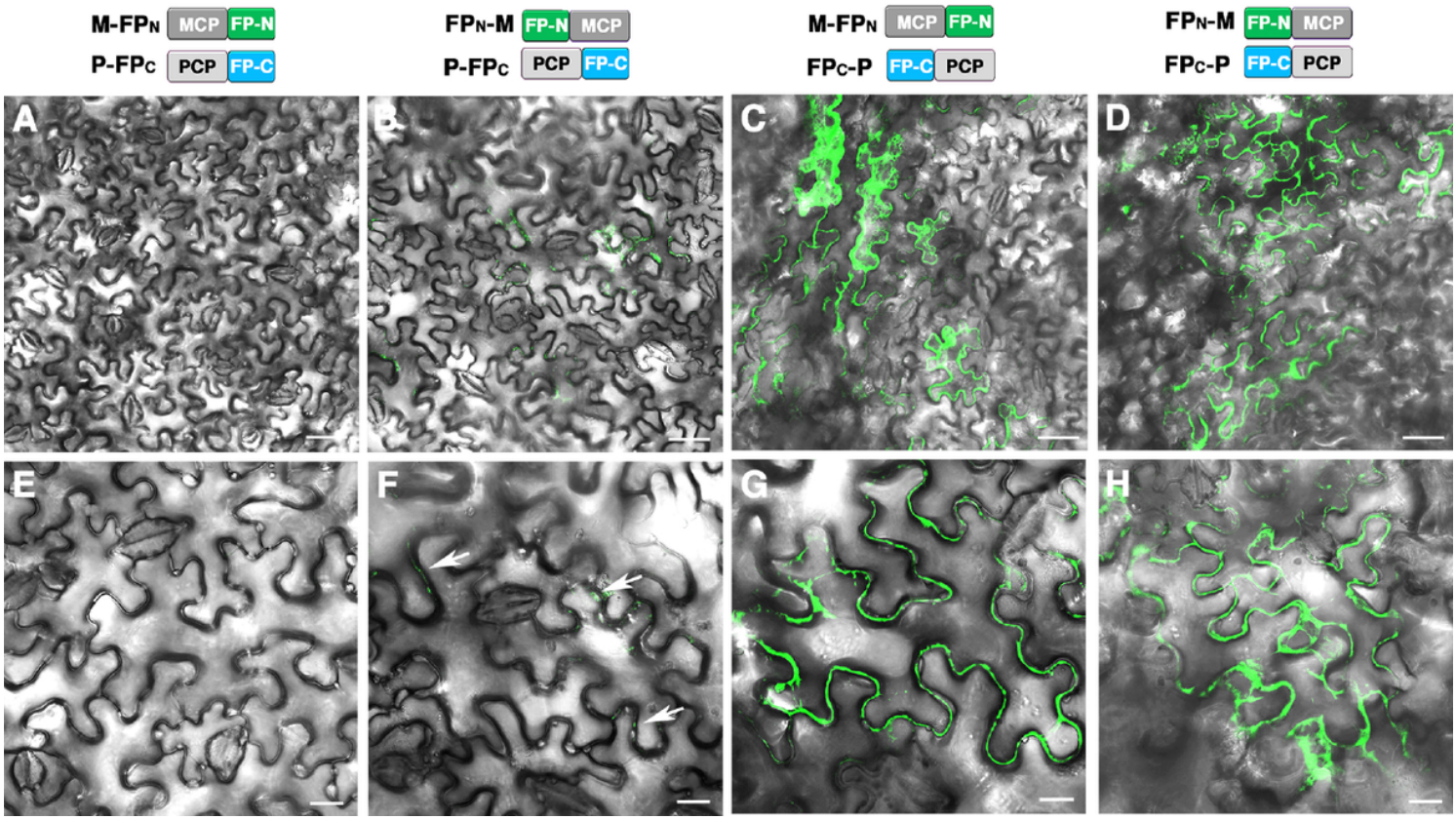


## Figure 4

GFP background fluorescence was not detected in cells with co-expression of M-FPN and P-FPC Confocal microscopy of N. benthamiana leaves co-infiltrated with (A, E) M-FPN and P-FPC; (B, F) FPN-M and P-FPC; (C, G) M-FPN and FPC-P; or (D, H) FPN-M and FPC-P. (E-H) Magnified images of (A-D). Note that background GFP is under the detection limit in (A, E). The weak background GFP fluorescence is indicated by white arrows in (F). Scale bar: (A-D) = 50 μm; (E-H) = 20 μm.

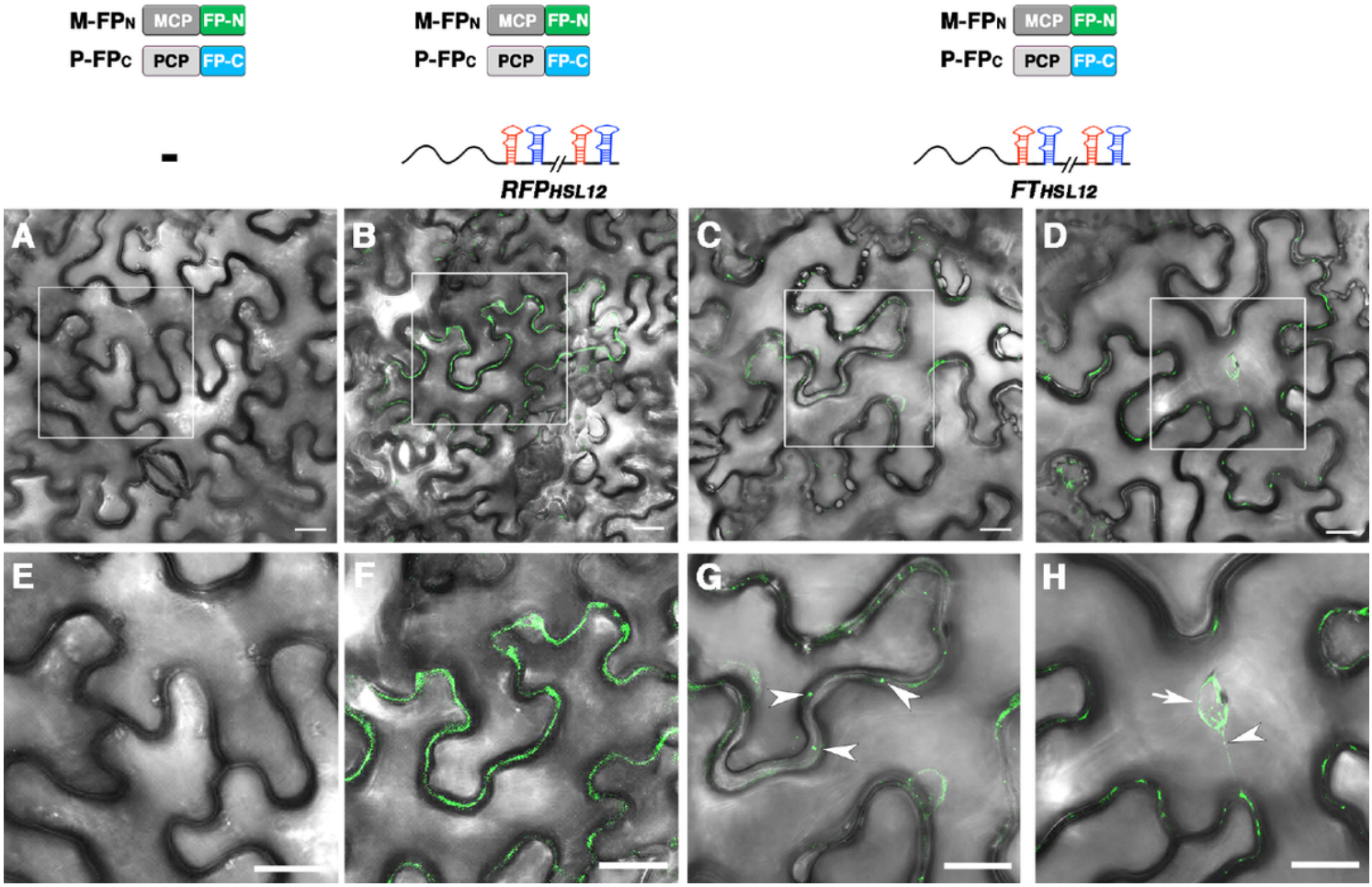


## Figure 5

Visualization of mRNA distribution by split fluorescent protein-based RNA live-cell imaging system Confocal microscopy of N. benthamiana leaves co-expressing (A, E) M-FPN and P-FPC without target mRNA; (B, F) M-FPN and P-FPC with RFPHSL12; or (C-D, G-H) M-FPN and P-FPC with FTHSL12 RNA. (E-H) are the magnified images of the rectangle marked area in (A-D). Different fluorescence distribution was detected in cells expressing RFPHSL12 or FTHSL12 RNA. (G) The puncta GFP fluorescence in the cell periphery is indicated by arrowheads. (H) The GFP fluorescence spot located on nucleus boundary or transported along cytoplasmic strands is indicated by an arrow or arrowhead, respectively. Scale bar = 20 μm in all images.

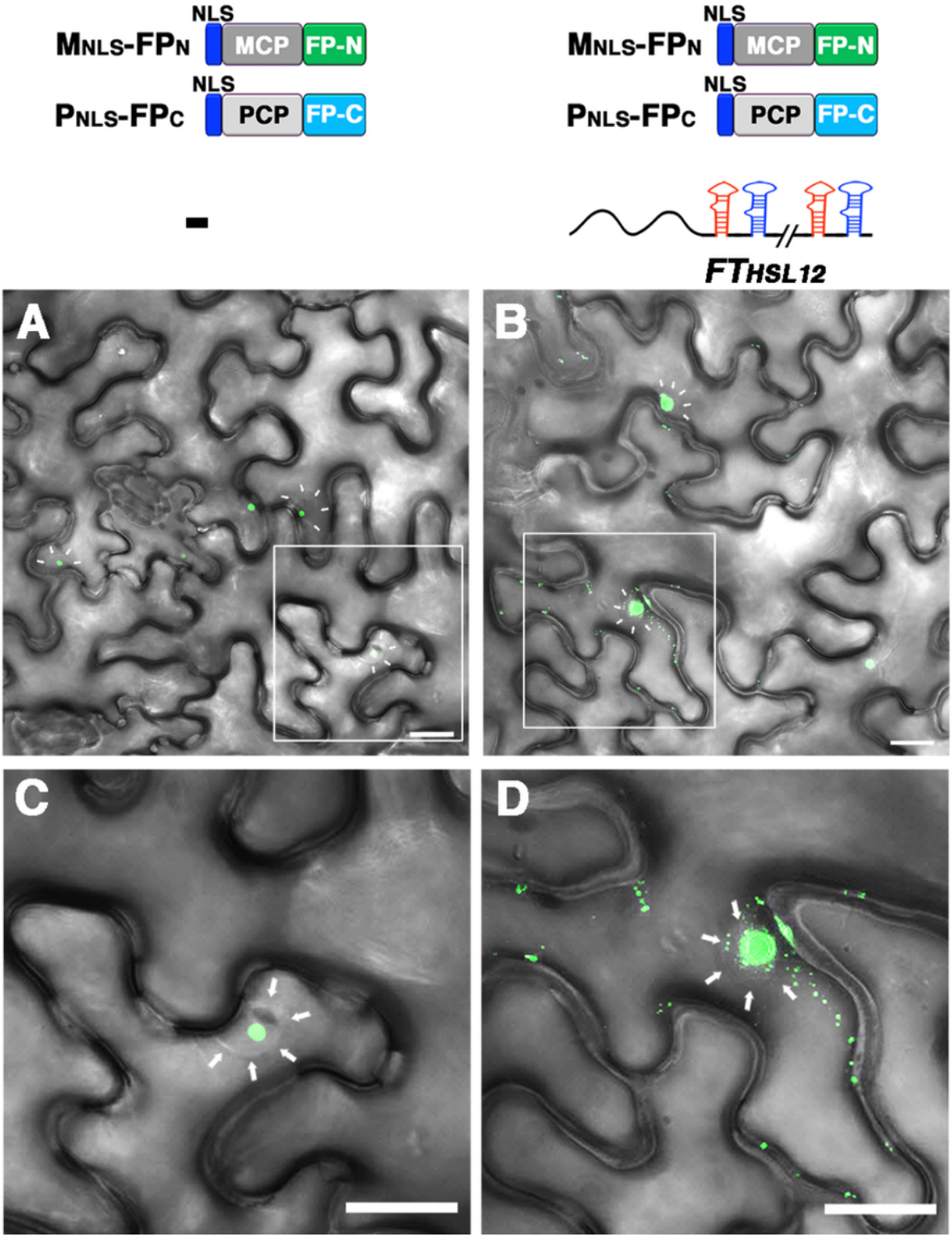


## Figure 6

Visualization of mRNA distribution in cells co-expressing MNLS-FPN and PNLS-FPC with FTHSL12 mRNA Confocal microscopy of N. benthamiana leaves co-expressing (A, C) MNLS-FPN and PNLS-FPC without target mRNA or (B, D) with FTHSL12. (C) and (D) are the magnified images of the rectangle marked area in (A) and (B), respectively. Note that the puncta fluorescence of FTHSL12 mRNA is detected along

cytoplasmic strands and cell periphery in (D). The boundary of the nucleus is indicated by arrows in (C and D). Scale Bar = 20 μm in all images.